Monte Carlo Simulation of Hole Transport in SiGe Alloys

Caroline S. Soares[1], Alan C. J. Rossetto[2], Dragica Vasileska[3], and Gilson I. Wirth[4]

[1,4]Caroline S. Soares and Gilson I. Wirth, Programa de Pós-Graduação em Microeletrônica, Universidade Federal do Rio Grande do Sul. Porto Alegre, Brazil
[2] Alan C. J. Rossetto, Centro de Desenvolvimento Tecnológico, Universidade Federal de Pelotas. Pelotas, Brazil
[3]Dragica Vasileska, School of Electrical, Computer and Engineering, Arizona State University. Tempe, USA
santos.soares@ufrgs.br

Abstract—**This paper employs the Ensemble Monte Carlo method to simulate the transport of holes in SiGe alloys. A three-band model was employed to describe the valence band of these alloys. The nonparabolicity and the warping effect of the heavy-hole and light-hole bands were considered in their dispersion relation, while the split-off band was described as parabolic and spherical. We consider phonon and alloy disorder scattering in these calculations. The mobility of holes for a range of SiGe alloys was calculated at 300K. The simulation mobility results agree with the experimental data, implying that the selected transport model for holes in SiGe alloys is adequate.**

Index Terms— **Ensemble Monte Carlo, hole transport, SiGe alloys, alloy disorder scattering, dispersion relation.**

I. Introduction

The progress in the microelectronic industry in the last 45 years has been guided by Moore's law [1]. However, the process of scaling down the transistor dimensions is expected to have a limit, which is established by quantum mechanics [2]. Because of that, other approaches are needed to enhance future improvements in the semiconductor industry. The approaches that are being proposed involve either changing the structure of the transistors or employing new materials or both [3].

Regarding use of new materials, p-type silicon-germanium transistors are found to be more reliable than conventional p-type silicon devices with respect to the Negative Bias Temperature Instability (NBTI) effect [4]. It has also been shown that holes have higher mobility in the SiGe alloy compared to pure silicon [5]. Hence, it is expected that SiGe alloys will replace pure silicon in the active channel region of the transistor. The SiGe alloys are semiconductors with electrical properties intermediate between those of silicon and germanium.

To successfully design future generations of transistors, the electrical properties, and the reliability of the transistors must be verified [6]. Hence, in the device development process, which is very time consuming and very expensive, modeling and simulation can significantly reduce the design to production time, thus reducing the cost. A Monte Carlo (MC) device simulator consists of a Poisson solver that is self-consistently coupled to a Monte Carlo charge carrier transport simulator [7]. In this work, an Ensemble Monte Carlo transport simulator is proposed and developed for simulation of hole transport in SiGe alloys. To simulate the dynamics of holes, effective mass description and scattering mechanisms due to lattice vibrations and alloy defects are used in our theoretical model.

II. Bulk Monte Carlo Model

Within the semiclassical transport theory, the Boltzmann Transport Equation (BTE) is solved to obtain the charge carrier distribution function [7]. The MC method is used to directly solve the BTE where the charge carrier is exposed to the action of the external forces due to the applied electric field and to the instantaneous scattering events. In the MC transport simulation, the time between two successive scattering events – the free-flight time – and the scattering mechanisms that terminate the carrier free-flights, are stochastically determined during the simulation [8]. When the movement of several charge carriers is tracked, the simulation is called Ensemble Monte Carlo (EMC). EMC device simulation is usually required in the analysis of semiconductor devices. For that purpose, a transport simulator for holes in SiGe bulk material is needed [8].

A. Band structure

The dispersion relation of the valence band is required to evaluate the scattering rates of holes in SiGe alloys and the energy and the velocity of holes. A three-band approach is used to model the valence band of SiGe alloys [9], [10], [11]. This model considers the heavy-hole, the light-hole and the split-off bands. The dispersion relation of the split-off band is defined as spherical and parabolic [9],[12]. In this work, we calculated the split-off band of SiGe alloys employing the Empirical Pseudopotential Method (EPM) [13]. The effective mass of the split-off band was extracted by fitting a parabolic equation to the EPM band structure data.

Both heavy-hole and light-hole bands of Si and Ge are anisotropic and non-parabolic [14]. Hence, heavy-hole and light-hole bands of SiGe alloys are also described as warped and non-parabolic bands. The dispersion relation of warped and non-parabolic bands equals the product of the dispersion relation for warped parabolic bands (which was proposed by Dresselhaus [15]) and the non-parabolicity function [14]:

$$E_H(k) = \frac{\hbar^2 k^2}{2m_0} \, |A|(1 - g(\theta,\phi))\chi_H \, ,$$
$$E_L(k) = \frac{\hbar^2 k^2}{2m_0} \, |A|(1 + g(\theta,\phi))\chi_L , \qquad (1)$$

where H and L refer to heavy-hole and light-hole bands, χ is the non-parabolicity function and $g(\theta,\phi)$ is given by

$$g(\theta, \phi) = \left[\frac{B^2}{A^2} + \frac{C^2}{A^2} q(\theta, \phi)\right]^{1/2} , \qquad (2)$$
$$q(\theta, \phi) = \sin^4\theta\cos^2\phi\sin^2\phi + \sin^2\theta\cos^2\theta \, ,$$

Digital Object Identifier 10.29292/jics.v16i1.156

where θ and ϕ are the polar and azimuthal angles in spherical coordinates of the reciprocal space. A, B and C are the Dresselhaus parameters of the material [14].

To obtain the Dresselhaus parameters, we used the EPM calculated heavy-hole and light-hole bands towards [100] and [111] directions, in a region near the gamma point. Neglecting the nonparabolicity effect in equation (1), Dresselhaus parameters were obtained by fitting the dispersion relation to the EPM data. Once the Dresselhaus parameters were extracted, we calculated the entire heavy-hole and light-hole bands using the EPM in both [100] and [111] directions. We estimated the nonparabolicity of both bands at each point in both directions, using [14]

$$\chi_H(E)=\frac{2m_0E(k)}{\hbar^2k^2|A|(1-g(\theta,\phi))},\quad \chi_L(E)=\frac{2m_0E(k)}{\hbar^2k^2|A|(1+g(\theta,\phi))}. \tag{3}$$

This resulted in a set of $\chi(E)$ for each band for both [100] and [111] directions. An average value of both energy and nonparabolicity, E_{av} and χ_{av}, was calculated to remove the directional dependence from the nonparabolicity function. The directional dependency of the dispersion relation is, therefore, only kept in the warping function [14].

The analytical expression of the nonparabolicity function is [14]

$$\chi(E)=\frac{aE^2+bE+c}{dE+1}. \tag{4}$$

This expression, proposed in [14], was chosen because its four parameters assure better agreement with the bands calculated using the EPM. Besides, the simplicity of the model makes its inclusion into the transport code easier. The parameters *a*, *b*, *c,* and *d* of each band were obtained by fitting equation (4) to the E_{av} and χ_{av} set of data. To achieve plausible results, we divided the energy range into small intervals, where each interval has a set of parameters that best fit the nonparabolicity function. After substituting the analytical function of the nonparabolicity in equation (1), the final expressions for the dispersion relations for the heavy-hole and the light-hole bands are:

$$E_H=\frac{\left(-bf_Hk^2+1\right)\sqrt{\left(bf_Hk^2-1\right)^2-4\left(af_Hk^2-d\right)cf_Hk^2}}{2\left(af_Hk^2-d\right)},\quad E_L=\frac{\left(-bf_Lk^2+1\right)\sqrt{\left(bf_Lk^2-1\right)^2-4\left(af_Lk^2-d\right)cf_Lk^2}}{2\left(af_Lk^2-d\right)}, \tag{5}$$

where f_L and f_H are related to the warping effect of the light-hole band and the warping effect of the heavy-hole band, respectively, and are calculated using

$$f_H=\frac{\hbar^2}{2m_0}|A|\left(1-g(\theta,\phi)\right),\quad f_L=\frac{\hbar^2}{2m_0}|A|\left(1+g(\theta,\phi)\right). \tag{6}$$

B. Scattering Mechanisms

Phonon scattering and alloy disorder scattering are the two most important mechanisms that must be accounted for when simulating the transport of holes in bulk SiGe [9], [10], [11]. In this work, we consider that the SiGe acoustic phonon spectrum is a single averaged branch of the pure materials. In contrast, the Si-like and the Ge-like modes coexist in the SiGe optical phonon branch. In this description, any phonon modes that could arise due to the alloy disorder have not been considered. The assumptions concerning the SiGe phonon branch have been supported by prior research findings [9], [11].

In the transport simulation, the scattering rate of each mechanism must be calculated to compute the free-flight time of each hole and to select the mechanism responsible for terminating the free-flights. In the EMC code, the scattering rates are stored in tables as a function of the hole energy.

The acoustic phonon transition rate considered in this paper is given in [16]. The acoustic phonon scattering is modeled as an elastic process that only causes intraband transitions, which is a reasonable approach when the transport simulation is performed at room temperature [17]. Phonons are assumed to be in equilibrium and described by Bose-Einstein statistics. In the elastic approximation there is no difference between the final state achieved by emission and absorption processes [16]. Therefore, the scattering rate of acoustic phonon is the sum of the emission and absorption scattering rates. The total scattering rate of the acoustic phonon mechanism as a function of the hole energy is given by

$$P_{HH}(E)=\frac{\sqrt{2}E_{ac}^2k_BT\langle m_H{}^{3/2}\rangle}{\pi\rho v_s^2\hbar^4}\sqrt{E}\mathcal{F}(E),\quad P_{LL}(E)=\frac{\sqrt{2}E_{ac}^2k_BT\langle m_L{}^{3/2}\rangle}{\pi\rho v_s^2\hbar^4}\sqrt{E}\mathcal{F}(E),\quad P_{SS}(E)=\frac{\sqrt{2}E_{ac}^2k_BT\left(m_{SO}{}^{3/2}\right)}{\pi\rho v_s^2\hbar^4}\sqrt{E}, \tag{7}$$

where ρ is the density of the material, T is the temperature of the material, E_{ac} is the acoustic coupling constant, v_s is the sound velocity in the material and $\langle m_H{}^{3/2}\rangle$ and $\langle m_L{}^{3/2}\rangle$ are the average effective masses, and are given by

$$\langle m_H{}^{3/2}\rangle=\frac{(m_0)^{3/2}}{4\pi|A|^{3/2}}\int_0^{2\pi}d\phi\int_0^{\pi}\frac{1}{\left(1-g(\theta,\phi)\right)^{3/2}}\sin\theta d\theta,\quad \langle m_L{}^{3/2}\rangle=\frac{(m_0)^{3/2}}{4\pi|A|^{3/2}}\int_0^{2\pi}d\phi\int_0^{\pi}\frac{1}{\left(1+g(\theta,\phi)\right)^{3/2}}\sin\theta d\theta, \tag{8}$$

and $\mathcal{F}(E)$ is given by

$$\mathcal{F}(E)=\frac{(dbE^2+2dcE-aE^2+c)E^{1/2}(dE+1)^{1/2}}{(aE^2+bE+c)^{5/2}}. \tag{9}$$

In the notation used for the total scattering rate, the first letter in the index of the total scattering rate refers to the initial and the second refers to the final band. Thus, HH corresponds to the intraband transition in the heavy-hole band, LL corresponds to the intraband transition in the light-hole band and SS corresponds to the intraband transition in the split-off band. To calculate the total scattering rate of acoustic phonon scattering of SiGe alloys, the acoustic coupling constant of SiGe alloys is obtained by linearly interpolating the values of pure Si and pure Ge [9].

The nonpolar optical phonon transition rate is given in [16]. The dispersion relation of the optical phonons responsible for the scattering is independent of the phonon wavevector [17], therefore, the frequency of the optical phonon is a

constant ω_{op}. The total scattering rate of the nonpolar optical phonon mechanism as a function of the hole energy is given by

$$P_{HH,LH,\,SH}(E)=\frac{\sqrt{2}D_{op}^{2}\langle m_H^{3/2}\rangle}{2\pi\hbar^3\omega_{op}}\begin{bmatrix}N_q\\N_q+1\end{bmatrix}\sqrt{E'}F(E')\,,$$
$$P_{LL,HL,\,SL}(E)=\frac{\sqrt{2}D_{op}^{2}\langle m_L^{3/2}\rangle}{2\pi\hbar^3\omega_{op}}\begin{bmatrix}N_q\\N_q+1\end{bmatrix}\sqrt{E'}F(E')\,, \quad (10)$$
$$P_{SS,HS,\,LS}(E)=\frac{\sqrt{2}D_{op}^{2}m_{so}^{3/2}}{2\pi\hbar^3\omega_{op}}\begin{bmatrix}N_q\\N_q+1\end{bmatrix}\sqrt{E'}\,,$$

where the upper terms correspond to the scattering rate due to the absorption and the lower terms correspond to the scattering due to the emission of an optical phonon. D_{op} is the optical coupling constant and E' is the final energy of holes and is given by $E'=E\pm\hbar\omega-\Delta E_{fi}$. The nonpolar optical phonon scattering in the SiGe alloys can be induced by Si-Si and Ge-Ge modes. Therefore, the scattering rate of each mode is weighted by the content of each atom in the alloy.

The alloy disorder scattering was also accounted for in simulating the transport of holes in SiGe alloys. The random distribution of the atoms that constitute random alloys is responsible for generating a perturbation that scatters the charge carrier while moving inside the alloy. The transition rate of the alloy disorder scattering is given in [18]. The total alloy disorder scattering rate as a function of the energy is given by

$$P_{HH,LH,SH}(E)=\frac{\Omega_0 2^{3/2}\langle m_H^{3/2}\rangle}{2\pi\hbar^4}\Delta U^2 x(1-x)\sqrt{E'}F(E')\,,$$
$$P_{LL,\,HL,SL}(E)=\frac{\Omega_0 2^{3/2}\langle m_L^{3/2}\rangle}{2\pi\hbar^4}\Delta U^2 x(1-x)\sqrt{E'}F(E')\,, \quad (11)$$
$$P_{SS,\,HS,\,LS}(E)=\frac{\Omega_0 2^{3/2}m_{SO}^{3/2}}{2\pi\hbar^4}\Delta U^2 x(1-x)\sqrt{E'}\,,$$

where Ω_0 is the volume of the unit cell, ΔU is the alloy scattering potential and x is the content of Ge in the SiGe alloy. In previous works, several values were attributed to the alloy scattering potential of SiGe alloys. In [9] and [11], a discussion concerning the lack of consensus about the value reported for the alloy scattering potential in the literature was made. This uncertainty may be a consequence of distinct expressions being employed to calculate the total scattering rate. They suggested considering the alloy scattering potential as a quantity to be empirically obtained. Another approach used in the literature is calculating the alloy scattering potential using first-principles methods. Both the virtual crystal approximation (VCA) or the coherent potential approximation (CPA) can be employed in tight-binding (TB) method to calculate the alloy scattering potential. In [19], an atomistic investigation was performed to calculate the alloy scattering potential. They calculated the TB band structure and wave function, and then extracted the alloy scattering potential. Comparing the empirically calculated alloy scattering potential and their results, they concluded that they were reasonably close. Because there is no relevant improvement in calculating the alloy scattering potential by first-principles methods, and first-principles calculations would increase the complexity of our model, the alloy scattering potential is a fitting parameter to reproduce the experimental mobility data.

III. Results

To validate the importance of alloy disorder scattering, the mobility of holes was calculated for low electric field and at 300K using the theoretical model described in the previous section. The obtained mobility data vs. Ge content were compared with experimental data [20] and previous theoretical calculations [11]. In [11], a full-band ensemble MC simulation was employed, where band structure calculations are performed during the simulation. The method employed in [11] is more computationally expensive than our model.

Table 1 presents the Dresselhaus parameters, the effective mass of the split-off band and the splitting energy of each SiGe alloy studied in this paper. These values were extracted from the band structure of each alloy calculated by EPM, following the methodology described in the previous section.

Table I. Parameters of the band structure of SiGe alloys simulated in this paper.

Ge content	*A*	*B*	*C*	m_{so} (m_0)	Δ (eV)
0.1	4.4	0.85	4.99	0.1408	0.05879
0.2	4.65	0.95	5.15	0.1402	0.08067
0.3	4.95	1.15	5.3	0.1356	0.1037
0.4	5.28	1.3	5.65	0.1282	0.1283
0.5	5.55	1.65	5.95	0.1189	0.1546
0.6	6.15	1.9	6.9	0.1086	0.1827
0.7	6.82	2.8	7.3	0.0982	0.2121
0.8	8.35	4.4	8.5	0.0889	0.2426
0.9	8.72	4.57	9.25	0.0812	0.2737

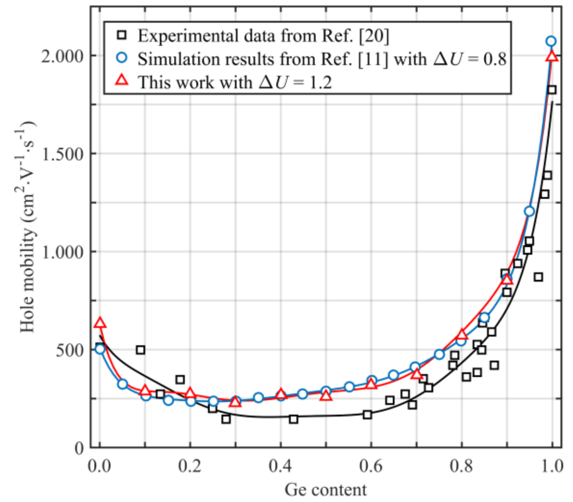

Fig.1 Comparison of the hole mobility in Si1-xGex alloys versus germanium content. The alloy scattering potential used in the in-house simulator is equal to 1.2. The interpolated lines are a guide to the eye.

Fig. 1 shows the experimental curve [20] and our simulation data when the alloy scattering potential was set to 1.2. Also shown in this figure is the simulation curve obtained by Fischetti and Laux [11] when using alloy scattering potential equal to 0.8. We can see a good agreement between the theoretical results. Comparing the theoretical results and the experimental data, we can observe that for the $Si_{0.8}Ge_{0.2}$ alloy the

mobility calculated agrees with the experimental value. However, for the other alloys, the experimental values are lower than the theoretical mobilities.

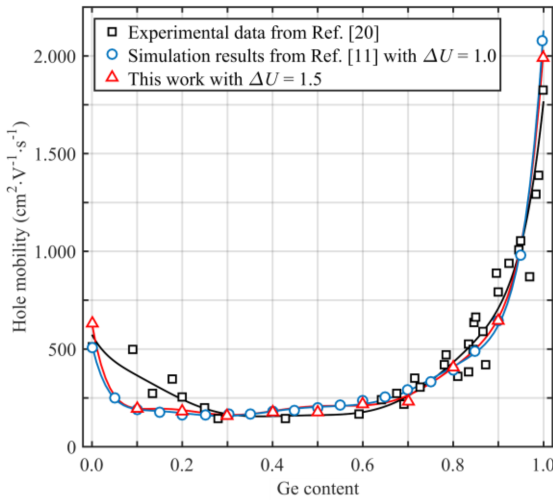

Fig.2 Comparison of the hole mobility in $Si_{1-x}Ge_x$ alloys versus germanium content. The alloy scattering potential used in the in-house simulator is equal to 1.5. The interpolated lines are a guide to the eye.

Following the suggestion given by Fischetti and Laux [11], the alloy scattering potential was slightly increased. Fig. 2 shows our mobility values when the alloy scattering potential is set to 1.5, the Fischetti and Laux [11] data for alloy scattering potential equal to 1, and the experimental data [20]. When the alloy scattering potential is set to 1.5, our simulated mobility data agree very well with both the experimental data and the results presented by Fischetti and Laux [11].

The profile of the mobility data vs. Ge content shows that the mobility of holes in alloys with low Ge content is smaller than the mobility of holes in Si. Nevertheless, when the Ge content is higher than 0.8, the hole mobility becomes larger in comparison with Si. This suggests that the impact of the scattering mechanisms on the hole mobility depends upon the Ge content.

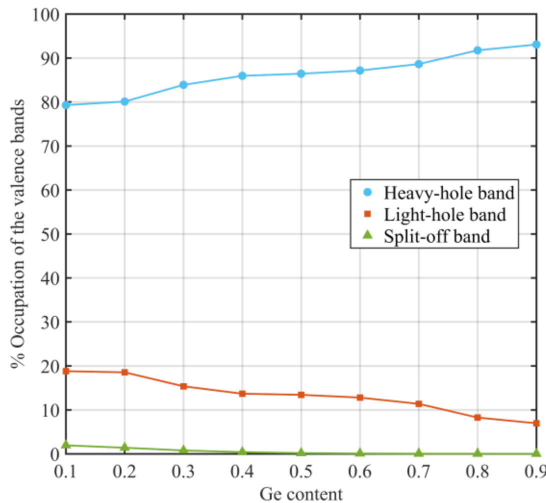

Fig.3 Occupation of heavy-hole band, light-hole band and split-off band versus Ge content. The lines are guide to the eye.

Fig. 3 shows the decrease of the occupancy of the light-hole band and the increase of the occupancy of the heavy-hole band as the Ge content increases. The split-off band is only slightly occupied in the entire Ge content range. Therefore, as the Ge content increases, the interband scattering is reduced (see [9] for more details). As a result, the mobility of holes in the heavy-hole band becomes more relevant than the mobility of holes in the light-hole band.

Fig. 4 shows the alloy disorder intraband scattering rates of heavy-hole band of $Si_{0.9}Ge_{0.1}$, $Si_{0.7}Ge_{0.3}$, $Si_{0.5}Ge_{0.5}$, $Si_{0.3}Ge_{0.7}$ and $Si_{0.1}Ge_{0.9}$ alloys as a function of energy, considering the energy range of interest for low electric fields. For low Ge content, the alloy disorder scattering rate increases as the Ge content increases reaching its maximum value for $Si_{0.5}Ge_{0.5}$, and then it starts to decrease. For high Ge content, the reduction of the heavy-hole band density of states is responsible for the decrease of the alloy disorder scattering rate.

In Fig. 5, we show the total phonon scattering rate as a function of the hole energy. For low Ge content, the acoustic phonon scattering is more likely to happen. Both the acoustic scattering rates and the Si optical phonon scattering rates are reduced as the Ge content increases, while the intraband non-polar optical scattering caused by Ge optical phonon becomes more relevant. Fig. 5 also shows that, for extremely low energy values, the total scattering rate increases with the Ge content. However, for values of energy higher than the thermal energy at 300K, the total phonon scattering rates become smaller as the Ge content increases. This trend is observed because, at extremely low energy, the acoustic scattering rate is low (but it rapidly increases with energy). This behavior is seen in the $Si_{0.9}Ge_{0.1}$, where the acoustic phonon scattering is more relevant than the optical phonon scattering (continuous green line in Fig. 5). The Ge optical phonon scattering rate slowly increases with the hole energy, and for the case of the $Si_{0.9}Ge_{0.1}$ alloy the Ge optical phonon scattering is more important than the acoustic phonon scattering.

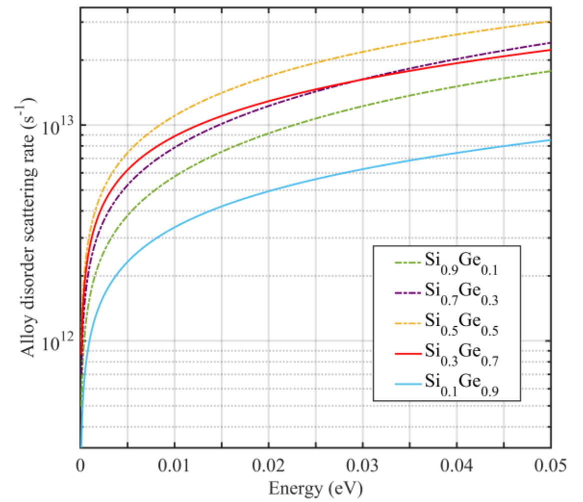

Fig.4 Alloy disorder scattering rate of $Si_{0.9}Ge_{0.1}$, $Si_{0.7}Ge_{0.3}$, $Si_{0.5}Ge_{0.5}$, $Si_{0.3}Ge_{0.7}$ and $Si_{0.1}Ge_{0.9}$. The alloy disorder scattering rates reaches its maximum value for $Si_{0.5}Ge_{0.5}$ and then decreases to reach its minimum value for $Si_{0.9}Ge_{0.1}$.

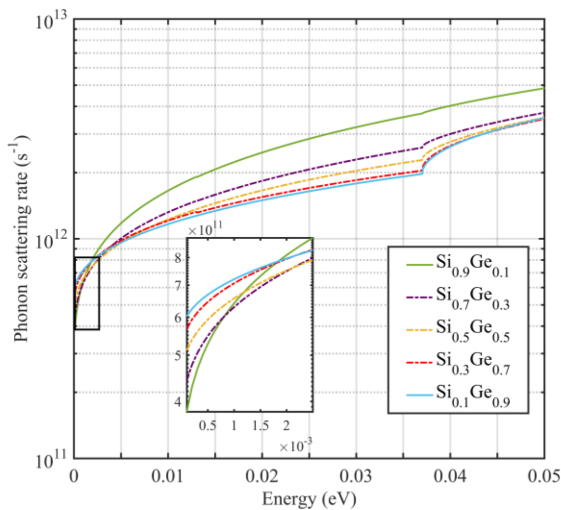

Fig.5 Phonon scattering rate of $Si_{0.9}Ge_{0.1}$, $Si_{0.7}Ge_{0.3}$, $Si_{0.5}Ge_{0.5}$, $Si_{0.3}Ge_{0.7}$ and $Si_{0.1}Ge_{0.9}$. The extremely low energy is depicted in zoom.

IV. Conclusion

The hole transport simulator for SiGe alloys was validated by calculating the low field mobility of holes in these alloys at 300K. The mobility estimated by this simulator was compared with previous simulation results and with available experimental data, thus demonstrating that the results obtained by the simulator are realistic and the presented theoretical model is adequate.

References

[1] G.E. Moore, "Progress in Digital Integrated Electronics", *Proc. Technical Digest Intel Electron Devices Meeting*, vol. 21, pp. 11–13, 1975.

[2] J. R. Powell, "The Quantum Limit to Moore's Law," *Proc. IEEE* 96, 1247 (2008).

[3] S. E. Thompson, R. S. Chau, T. Ghani, K. Mistry, S. Tyagi and M. T. Bohr, "In Search of "Forever," Continued Transistor Scaling One New Material at a Time" *IEEE Transactions on Semiconductor Manufacturing*, vol. 18, no. 1, february 2005

[4] J. Franco, et al. "On the impact of the Si passivation layer thickness on the NBTI of nanoscaled Si0:45Ge0:55 pMOSFETs". *Microelectronic Engineering*, v. 88, n. 7, p.1388–1391, 2011.

[5] S. Kasap and P. Capper, *Springer Handbook of Electronic and Photonic Materials*. Springer**,** 2006

[6] H. Chenming, "IC Reliability Simulation", *IEEE Journal of Solid-State Circuits*, vol. 27, n. 3. March 1992.

[7] D. Vasileska and S. M. Goodnick, *Computational Eletronics*. Materials science and Engineering. R 38, p. 181-236, 2002.

[8] C. Jacoboni and L. Reggiani, "The Monte Carlo method for the solution of charge transport in semiconductors with applications to covalent materials," *Rev. Mod. Phys*., vol. 55, pp. 645–705, Jul 1983.

[9] P. J. Briggs, A. B. Walker and D. C. Herbert, "Calculation of hole mobilities in relaxed and strained SiGe by Monte Carlo simulation" *Semiconductor Science and Technology*, [s.l.], v. 13, p. 680-691, 1998.

[10] J. M. Hinckley and J. Singh, "Hole transport theory in pseudomorphic $Si_{1-x}Ge_x$ alloys grown on Si(001) substrates", *Physical Review B*, vol. 41. n. 5. February, 1990.

[11] M. V. Fischetti and S. E. Laux, "Band structure, deformation potentials, and carrier mobility in strained Si, Ge, and SiGe alloys". *Journal Of Applied Physics*, [s.l.], v. 80, n. 4, p.2234-2252, 15 August 1996.

[12] K. Kano, *Semiconductor Devices*. New Jersey: Prentice Hall, 1998.

[13] S. Gonzalez Empirical pseudopotential method for the band structure calculation of strained Si1-xGex materials. Thesis (Master of Science) - Arizona State University, Tempe, AZ, 2001.

[14] S. Rodríguez-bolívar, F. M. Gómez-campos and J. Carceller, "Simple analytical valence band structure including warping and non-parabolicity to investigate hole transport in Si and Ge". *Semiconductor Science and Technology*, [s.l.], v. 20, n. 1, p.16-22, 27 nov. 2004.

[15] G. Dresselhaus, A. F. Kip and C. Kittel. "Cyclotron Resonance of Electrons and Holes in Silicon and Gerii1anium Crystals". *Physical. Review*, [s.l.], v. 98, n. 2, p. 368-384, 1955.

[16] C. Jacoboni and P. Lugli, *The Monte Carlo Method for Semiconductor Device Simulation.* Springer. 1989

[17] C. Jacoboni, *Theory of Electron Transport in Semiconductors: A Pathway from Elementary Physics to Nonequilibrium Green Functions*. Springer, 2010.

[18] J. W. Harrison and J. R Hauser, "Alloy scattering in ternary III-V compounds". Phys. Rev. v. 13, 1976.

[19] S. R. Mehrotra, A. Paul and G. Klimeck. "Atomistic approach to alloy scattering in Si1−xGex" *Appl. Phys. Lett*. 98, 173503, 2011.

[20] G. Busch and O. Vogt. "Elektrische Leitfähigkeit und Halleffekt von Ge-Si-Legierungen". *Helvetica Physica Acta.* v. 33. p. 437-458,1960.